Flexible and Printed Electronics

PAPER

RECEIVED
6 June 2016

REVISED
25 August 2016

ACCEPTED FOR PUBLICATION
29 August 2016

PUBLISHED
23 September 2016

# Silver nanowires in poly(methyl methacrylate) as a conductive nanocomposite for microfabrication

**Eduardo D Martínez**[1], **Javier H Lohr**[2], **Martín Sirena**[2], **Rodolfo D Sánchez**[2] **and Hernán Pastoriza**[1]

[1] División Bajas Temperaturas, Centro Atómico Bariloche, Comisión Nacional de Energía Atómica. Av Bustillo 9500, S. C. Bariloche, R8402AGP, Río Negro, CONICET, Argentina

[2] División Resonancias Magnéticas, Centro Atómico Bariloche, Comisión Nacional de Energía Atómica. Av Bustillo 9500, S. C. Bariloche, R8402AGP, Río Negro, CONICET, Argentina

**E-mail:** edmartin@cnea.gov.ar

**Keywords:** silver nanowires, microfabrication, electron beam lithography, soft lithography, nanocomposites, flexible electronics

Supplementary material for this article is available online

## Abstract

A novel nanocomposite resist is presented based on AgNWs dispersed in poly(methyl methacrylate). It is shown that this nanocomposite resist displays sheet resistances below 10 $\Omega$ sq$^{-1}$ for concentrations of AgNWs higher than 4%wt and can be used for a wide range of microfabrication techniques. The resist can act as a conductive ink that cures at room temperature, form thin films with low sheet resistances, and be used in fast replication methods derived from soft lithography. Furthermore, it can be applied for nano-scale fabrication via electron beam lithography (EBL) on different substrates, including flexible and insulating materials, providing a straightforward method to avoid charging effects. This, being the first report about a nanocomposite resist based on AgNWs for EBL, describes a simple procedure to account for suspended nanowires, forming bridges, nanocantilevers and more complex nanostructures. A wide range of opportunities opens for the single-step fabrication of electronic components in the nano and micro scale.

## 1. Introduction

Much work has been performed lately regarding transparent conductive layers for their use in flexible electronics and devices such as touch screens, displays and solar cells. The traditional material used as transparent conductor, indium tin oxide (ITO), fails in these applications due to its mechanical properties and needs to be replaced [1]. Silver nanowires (AgNWs) are probably the most promising materials to achieve this goal due to the highest conductivity of silver among metals ($1.6 \times 10^{-8}$ $\Omega$ m) and the large aspect ratio of nanowires attainable during synthesis [2]. Conductive networks with low metal fraction content, therefore practically transparent, are possible by using AgNWs [3, 4]. This concept has recently been investigated for solar cell technologies as a straight forward method to replace ITO as the transparent electrode [5–7]. On the other hand, nano and microfabrication through top-down approaches make common use of polymer based resists for optical and electron beam lithography (EBL). However, polymers are mainly employed as sacrificial materials, while others (metals, semiconductors and oxides) are used as structural components of devices. Moreover, since the most common transduction mechanism of nano- and micro-electromechanical systems and sensors is electrical, conductive materials need to be present in the device. Therefore, processes such as evaporation and sputtering of metals, followed by lift-off, are commonly employed, imposing additional fabrication steps and increasing the final cost of devices. The development of an electrically conductive resist would provide a straightforward method to fabricate in a one-pot procedure a wide variety of devices and components such as resistors, connectors, capacitors and so on. Some attempts have been performed so far in this regard, and a variety of nanoparticle-polymer photoresist composites had been reported for microfabrication [8, 9]. Nanoparticles with magnetic [10, 11], metallic [12, 13] and semiconducting [14, 15] properties have been mixed with photoresists to develop novel nanocomposite materials for microfabrication. It is worth to mention that silver/polymers

nanocomposites are being studied as well for other applications such as catalysis [16], dry electrodes for medical sensing [17], antibacterial coatings [18] and heating elements for therapy [19], among others [20]. For electrically conductive photoresists, the most frequently studied fillers so far are carbon black [21], carbon nanotubes [22–24] and silver nanoparticles [13]. However, all of these systems present serious difficulties regarding scalability and processing.

In this work, we present a nanocomposite material with high electrical conductivity, low filler content, and remarkable processing properties. This novel material can be easily applied in the fabrication of microdevices through different techniques. We show that the nanocomposite resist can be used for EBL making it possible to extend the usage of this technique over insulating materials, such as polymers and glass, avoiding the charging effect that severely limits EBL [25–27]. Also, microfabrication of electrically conductive devices can be performed with this material by applying soft lithography techniques such as nanoimprint lithography [28]. This resist can even be used as a conductive ink that cures at room temperature.

## 2. Experimental details

### 2.1. Synthesis of Ag nanowires

Long AgNWs were synthesized by adapting a one-pot polyol procedure following Jiu *et al* [29]. In a borosilicate flask, 0.8 g of polyvinylpyrrolidone (PVP, Mw = 360000 g mol$^{-1}$) were slowly dissolved in 50 ml of anhydrous ethylenglycol (EtGOH, Sigma-Aldrich); in a second flask, 1.0 g of $AgNO_3$ was dissolved in 40 ml of EtGOH. After complete dissolution, both solutions were mixed and 13.6 g of a 0.6 mM solution of $FeCl_3 \cdot 6H_2O$ in EtGOH were added. This preparation was introduced in a 500 ml sealed round flask and placed into a pre-heated bath at 130 °C for 5 h without stirring. The obtained particles were extracted by adding acetone in a 1:4 volume ratio followed by centrifugation at 4000 rpm for 5 min. The supernatant was then removed and the NWs were dispersed in isopropanol by vortex agitation and a short pulse of ultrasonication (40 kHz, 160 W). Sonication time was limited since it can severely damage the AgNWs integrity. These washing steps were repeated four times in total. In the final step, the supernatant was removed and the residual AgNWs were dried under a constant flux of $N_2$.

### 2.2. Electron beam lithography

EBL was performed using a Philips XL30 SEM with a $LaB_6$ filament. NPGS system was employed to control the exposure and externally control the stage positioning. Exposure doses were varied from 200 to 500 $\mu$C cm$^{-2}$. Development was performed after exposure using 1:3 volume mixture of methyl isobuthyl ketone: isopropanol (MIBK:IPA) for 70 s at room temperature. Etching of the exposed AgNWs was made with $NH_4OH$:$H_2O_2$ 1:1 v:v. for 90 s.

### 2.3. Nanomanipulation

Inside the Philips XL30 SEM chamber, four tungsten probes were mounted on a Zyvex S100 Nanomanipulator System able to perform controlled movements in steps of 5 nm resolution. The current–voltage ($I$–$V$) curves were acquired using this device and a Keithley 4200-SCS (semiconductor characterization system). The tungsten probes used were previously prepared by electrochemical etching method in a home made setup, which include: tungsten wire as working electrode, Ag/AgCl as reference electrode, Pt as counter electrode and a TQ-04 potentiostat. To perform the needles, the working electrode was fixed in a micrometer screw, which was positioned and extracted (during the etching) with a step motor. To avoid the native oxide coating on the tips, these were successively cleaned with deionized water (DIW), 0.07 M of KOH, isopropyl solution and DIW again. Inside the SEM chamber and before the measurements, a cleaning procedure was performed in which the tips in pairs are crossed and the electrical current is increased in steps until a resistance of around 10–20 Ω is reached.

### 2.4. Conductive-tip AFM

Topography and conductivity measurements were performed at room temperature on a Bruker 'Dimension 3100' conductive-tip scanning probe microscopy (CT-AFM) with an 'Extended TUNA' module from Bruker Corporation. Boron-doped diamond conductive tip ('DESP' probes from Bruker) with a spring constant between 20 and 80 N m$^{-1}$ were used. The minimum detectable current in the CT-AFM is 50 fA and the maximum current limit is 1 $\mu$A, under a bias voltage ranging from 0.01 to 12 V. All CT-AFM measurements were performed at room temperature and maintaining the same value of deflection setpoint (force exerted on the sample surface of 0.5 V). The measurements were perform in 'virgin' areas of the sample's surface (non-scanned areas) to reduce the chemical modification of the surface due to the tip polarization voltage and to avoid damaging the sample.

### 2.5. Profilometry

Film thickness of shown samples were obtained using a stylus profilometer Alpha-Step, Tencor Instruments inc.

## 3. Results and discussion

Extracted AgNWs have a mean size of 40 $\mu$m in large and diameters between 150 and 250 nm as shown in the online supplementary information (SI), figure S1. For the preparation of nanocomposite resists,

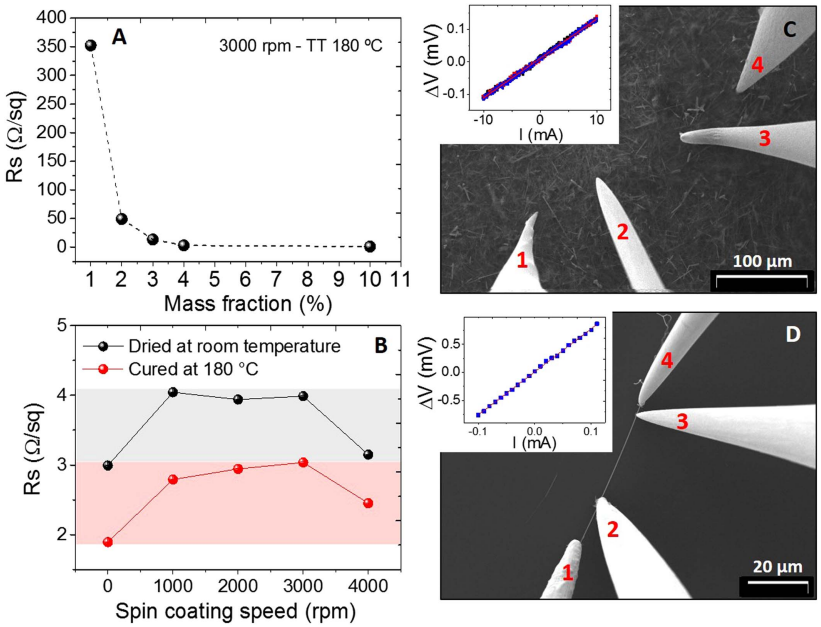


**Figure 1.** (A) Sheet resistance of AgNWs-PMMA nanocomposite resist with different silver mass fraction after curing at 180 °C. (B) Sheet resistance of 4.0%wt AgNWs-PMMA deposited by drop casting (0 rpm) and spin coating at different spinning speeds before and after curing at 180 °C. (C) Local measurement of *I–V* curves obtained by 4-probe nanomanipulation on the nanocomposite film and (D) on a single AgNW.

weighted amounts of AgNWs were dispersed in a mixture 1:3.64 m:m of IPA and PMMA-C4 (Mw = 950000 g mol$^{-1}$ 4.0%wt in chlorobenzene, MicroChem). Colloids with different silver mass fraction were prepared by this way and homogeneous mixtures were achieve by vortex agitation. Although the stability of the colloids is limited in time because of the high mass of the AgNWs, redispersion of decanted nanowires can be easily performed by strong manual or vortex agitation. As mentioned before, ultrasonication should be avoided or, at least, should be limited.

### 3.1. Electrical properties

For the characterization of the bulk electrical properties, pre-patterned substrates with four-probe electrodes were made on glass cover slides by optical lithography using the positive tone resists Shipley S1800 Microposit, followed by sputtering of gold/copper 70/30 alloy and lift-off. Designed electrodes consisted in equally spaced rectangles (4 mm large, 2 mm wide and 1 mm gap). The formulated AgNWs-PMMA nanocomposite resist was used to form thin films via spin coating and drop casting. In the spin coating case, deposition of the nanocomposite resist with different silver concentrations was performed at 3000 rpm (figure 1(A)). The drying process was very fast and occurred mainly during spinning. The bulk sheet resistance ($R_s$) of the dry films presented a sharp reduction for concentrations of silver in the nanocomposite resist higher than 2.0%wt, reaching a lower limit value of (1.6 ± 0.5) Ω sq$^{-1}$ for concentrations of silver higher than 4.0%wt. Resistance values did not change appreciably after two minutes of rest at room temperature after spinning. For the case of films deposited by drop casting the drying can take up to ten minutes. At higher concentrations of AgNWs in the resist the resistance of the samples is lower due to the increasing number of conduction paths. Another set of samples was prepared at different spinning velocities of 1000, 2000, 3000 and 4000 rpm using the nanocomposite resist with 4.0%wt of silver. Thicknesses ranged from 4.0 to 2.5 $\mu$m from lower to higher spinning speeds, although surface roughness of samples imposed an error of 0.5 $\mu$m in each case. The film prepared by drop casting resulted in a final thickness of (20 ± 3) $\mu$m. Figure 1(B) shows that $R_s$ of the films remains constant for intermediate spinning speeds ($S_s$, rpm) ($1000 < S_s < 3000$). However, for higher spinning speeds $R_s$ decreases, probably due to compression of the AgNWs network because of the stronger centrifugal forces acting during spinning. It is interesting to note that $R_s$ of the films decreases after annealing. In all cases, the electrical conductivity was studied before and after curing at 180 °C. A sheet resistance reduction of about 30% was found after thermal treatment. The film contraction and the reduction of the mean distance between nanowires could be factors that effectively increase the conduction pathways.

The electrical properties at the nano and microscale were studied using 4-probe nanomanipulation (see figure 1(C)) inside the main chamber of the SEM. In this set of experiments, local conductivity of the resist was analyzed by placing in line four tungsten needle-shaped probes at close positions on a thin film made by spin coating at 3000 rpm and cured at 180 °C

from a AgNWs-PMMA nanocomposite resist with 4.0%wt of AgNWs. Current injection was controlled through outer needles (numbered 1 and 4) while voltage drop was measured between probes located in the middle region (needles 2 and 3). Ohmic contact i.e. linear relation between current and voltage was observed. Resistivity ($\rho$) and sheet resistance, $R_s$, were calculated using a 4-probe model with point-like contacts based on the following equation [30]

$$\rho = R_s t = 2\pi\frac{V}{I}[s_1^{-1} - (s_1 + s_2)^{-1} - (s_2 + s_3)^{-1} + s_3^{-1}]^{-1}, \quad (1)$$

where $t$ is the film thickness, and $s_1$, $s_2$ and $s_3$ are the gap distance between needles 1 and 2, 2 and 3 (voltage sensing) and 3 and 4 respectively. It was noticed that soft contact between probes and the resist surface was insufficient to achieve ohmic contact and the probes had to be nailed down, exerting pressure on the film. Only then, good electrical contact was obtained.

In addition, resistivity measurements of a single nanowire were also performed using nanomanipulation by placing 4-probe needles on an isolated AgNW. Silicon wafer covered by native $SiO_2$ layer was used as substrate. *I–V* curves were acquired: (i) first, on the bare substrate confirming electrical isolation, and (ii) on a single AgNW of $(290 \pm 20)$ nm in diameter and $(30.2 \pm 0.4)$ $\mu$m in length (figure 1(D)). Resistance was extracted from the linear slope obtaining $R = (7.72 \pm 0.05)$ $\Omega$, representing a nanowire resistivity $\rho = (1.7 \pm 0.2) \times 10^{-8}$ $\Omega$ cm, in excellent agreement with bulk silver resistivity.

To better understand the percolation of the AgNWs network, CT-AFM was employed for the characterization of both the topography and the current profile. A copper/gold electrode was deposited by sputtering on glass substrates and the nanocomposite films were spin-coated on top of them at 3000 rpm from the AgNWs-PMMA nanocomposite resists with two different AgNWs concentration: 4.0%wt and 0.4%wt. A voltage difference of 1 V was applied between the tip of the CT-AFM and the electrode in order to measure the current profile in the vertical direction, i.e. perpendicular to the substrate. As the conductivity of silver is high enough to saturate the current detected by the CT-AFM equipment (maximum current 1 $\mu$A) the current profile was basically an ON–OFF map of the conductivity in the scanned area (figures 2(B) and (D)). Interestingly, when comparing the deflection of the cantilever and the current profile for 4.0%wt AgNWs-PMMA films (figures 2(A) and (B)) it is evident that the majority of the nanowires observed in the deflection profile match with the saturated current profile, showing they are electrically connected with the bottom electrode. However, there are a minor fraction of AgNWs that become observable in the topography profile but do not appear as conductive hot-spots in the current profile. For the film deposited from a nanocomposite resist with ten times less concentration of AgNWs (0.4%wt), this observation is more evident and most of the AgNWs perceived in the topography do not show electrical percolation to the substrate as shown in figures 2(C) and (D). Therefore, percolation is not guarantied for all nanowires and a percolated network depends, as expected, with the concentration of AgNWs in the nanocomposite resist. Of course, the AgNWs that appear in the deflection profile are the ones located close to the top surface of the film, or even emerging from it, but in any case they are only a fraction of the total amount of nanowires present below the surface, as will be shown in the next section. Also, an insulating layer of polymer between the sub-surface nanowires and the conductive tip could avoid electrical contact but show deflection anyway. It is remembered here that the film has a thickness of c.a. 3 $\mu$m while the AgNWs have a mean diameter of 200 nm. Therefore, in order to show conduction, either the AgNWs need to be tilted and reaching both the surface and the bottom electrode, or else, a percolation must be formed involving several AgNWs in electrical contact (see also SI for topography plots obtained by CT-AFM, figure S2).

### 3.2. Patterning techniques

In order to test if the conductive AgNWs-PMMA resist is suitable for its use in microfabrication, patterns of the nanocomposite resist were made by two different techniques: EBL and soft-lithography. While EBL is well established technique used for low scale production of nano and microstructures, it is typically applied over conductive materials using polymeric resists that act as sacrificial materials, which are finally removed. The spatial resolution can be as low as tens of nanometers. On the other hand, soft-lithography, introduced in the late 90s by Xia and Whitesides [31], is a highly versatile technique. New variations and derived methods are constantly reported. So far, soft-lithography main derived techniques are nanoimprint lithography, micro contact printing, micro transfer printing and replica molding [28]. Soft lithography, contrary to EBL, can be performed on large areas and industrial quantities, both on insulating and flexible substrates and with submicrometric spatial resolution. However, soft lithography derived techniques require the fabrication of a master sample by any other method, which is used to make an inverse replica using an elastomer, typically poly(dimethyl siloxane) (PDMS). Schematics of both processes are displayed in figure 3.

In the first case, films of the resist with 4.0%wt of silver were deposited by spin coating at 3000 rpm and baked at 180 °C for 2 min before exposure to the electron beam. This procedure was identical to the standard protocol used for EBL of PMMA resists, using an exposure dose of 300 $\mu$C cm$^{-2}$ and a development time of 70 s in MIBK:IPA 1:3 volume mixture. Interestingly, the regions exposed to the electron beam,

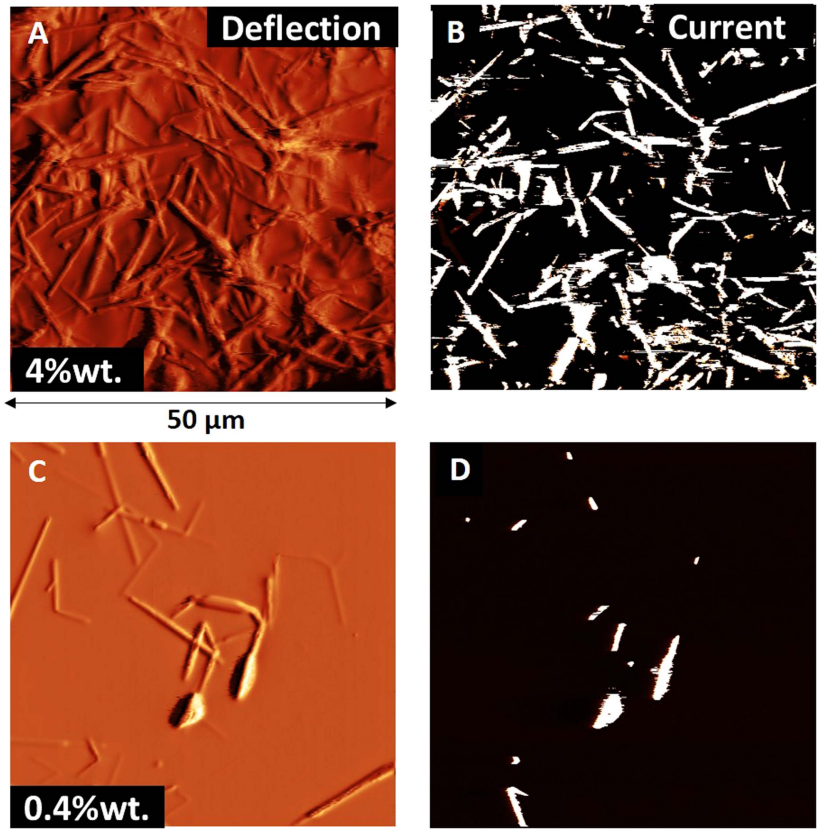


**Figure 2.** CT-AFM measurements of AgNWs-PMMA resist. Left panels: topography shown as the deflection of the conductive tip; right panels: current profile of a nanocomposite film deposited at 3000 rpm from 4.0%wt (A), (B) and 0.4%wt (C), (D).

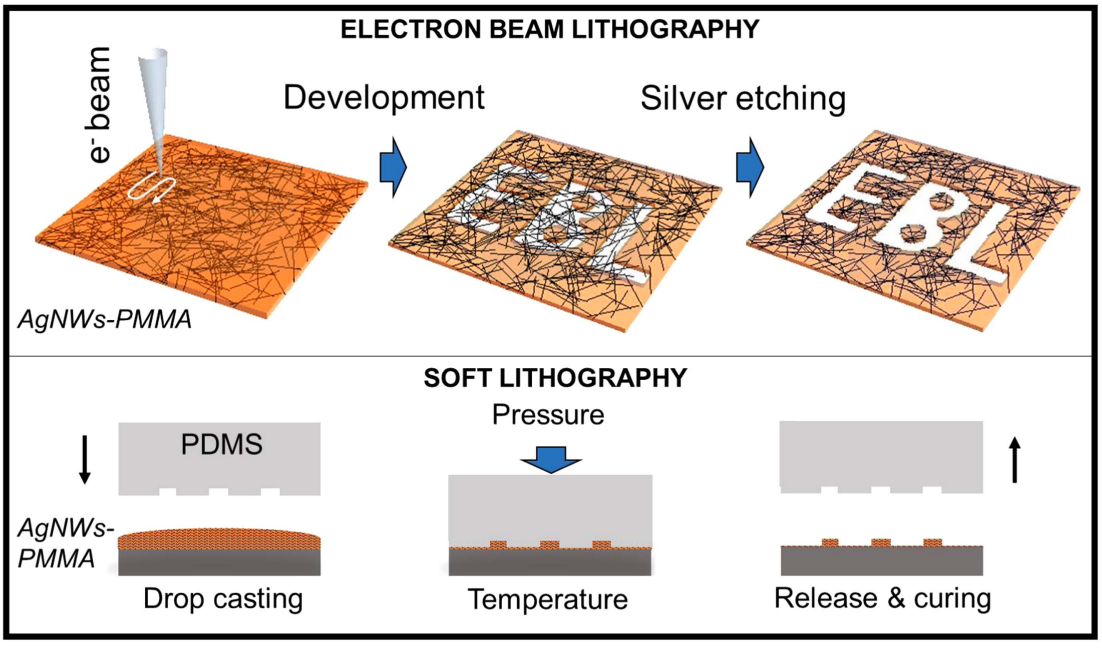


**Figure 3.** Microfabrication processes applied to the nanocomposite resist. Top: EBL directly applied on the AgNWs-PMMA resist after spin coating over insulating or conductive substrates. After exposure, the development of the PMMA resist followed by the wet etching of the uncovered silver are performed. Bottom: soft lithography technique applied on the modified resist deposited by drop-casting over flexible or rigid substrates.

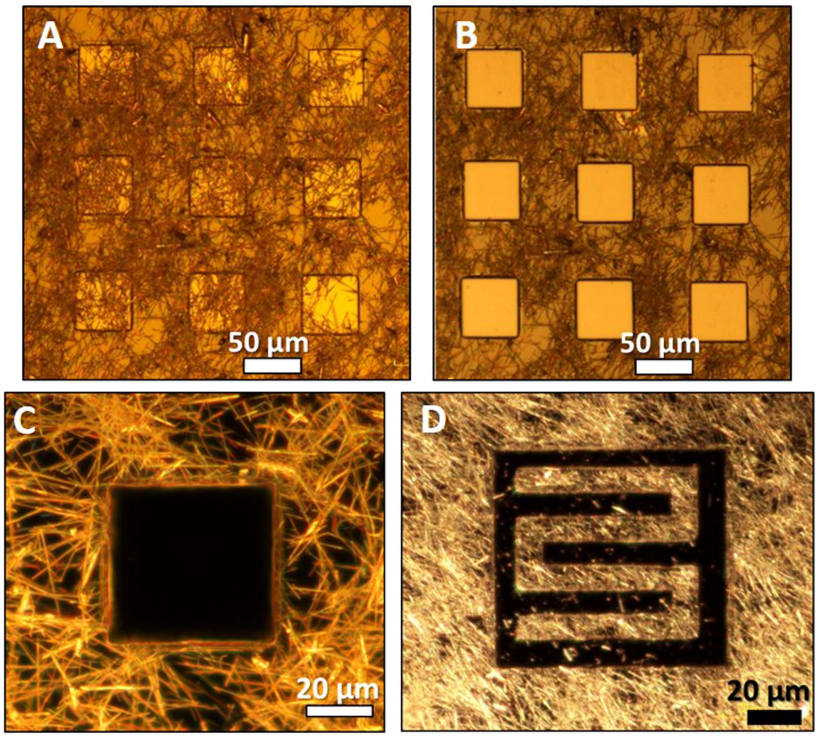


**Figure 4.** Optical image of EBL patterns before (A) and after (B) silver etching. (C), (D) Dark field optical image of EBL patterns after silver etching.

when developed, reveal the underneath network of AgNWs (figure 4(A)). This provides a direct and simple method to achieve suspended nanowires forming bridges and cantilevers. On the other hand, if such structures are not desired and only the patterns are sought, the exposed AgNWs can be removed by wet chemical etching of silver using a 1:1 volume mixture of concentrated $NH_4OH$:$H_2O_2$ for 90 s (figures 4(B), (C) and (D)). The etching time was found to be important because the dissolution of AgNWs can advance into the inside of the PMMA covered regions by lateral etching of AgNWs (see online SI, figure S3).

Insulating materials like glass, silicon nitride ($Si_3N_4$) and polymers such as polyimide were also tested as suitable substrates, finding acceptable and comparable results. It is worth to mention that the adhesion of the nanocomposite resist on different materials is a key factor to have into account. For the case of glass, the adhesion was observed to improve after two minutes exposure to an oxygen plasma cleaning treatment before the deposition of the resist. Similar improvement in the adhesion was observed for polyimide films. The second requirement for performing EBL on insulating substrates is the necessity of contacting the conductive nanocomposite film with the metallic stub or holder to allow for the discharge of the electron beam. This was made by using a thin stripe of carbon tape contacting a corner of the film to the holder. Taking these precautions, EBL can now be performed on insulating materials without the electrical charging of the surface. Examples of EBL on these insulating substrates after the plasma treatment are shown in figure 5.

Additional examples of the capabilities of the nanocomposite resist for EBL are shown in figure 6, where EBL was used to reveal the underneath AgNWs network of the resist (figure 6(A)), produce strips of different widths (figure 6(B)), sustain laterally emerging AgNWs (figure 6(C)), achieve suspended AgNWs forming bridges and floating networks (figure 6(D)), manually cover or uncover specific regions of a single nanowire (figures 6(B) and (F) inset).

For the case of soft lithography, a master with a resistor pattern consistent of 100 $\mu$m wide tracks was first made. Negative photoresist SU-8 2010 (Microchem corp.) deposited on glass was processed by regular photolithography in order to pattern the designed feature. Replica molds, to be used as soft lithography stamps, were made using PDMS (Sylgard 184, Dow Corning) following standard methods [32]. To produce conductive tracks with the nanocomposite resist, a small volume of it was drop on different substrates, the PDMS stamp was applied and pressed tightly until the resist was dry, then the mold was carefully removed. An inverted replica of the stamp was obtained with regular features. It was cured at 180 °C for 2 min. The best adhesion performance was obtained on PET films, providing a simple method to achieve conductive patterns on flexible and transparent substrates in a single step. Optical images of the device are shown in figures 7(A), (C) and (D). Conductivity of the

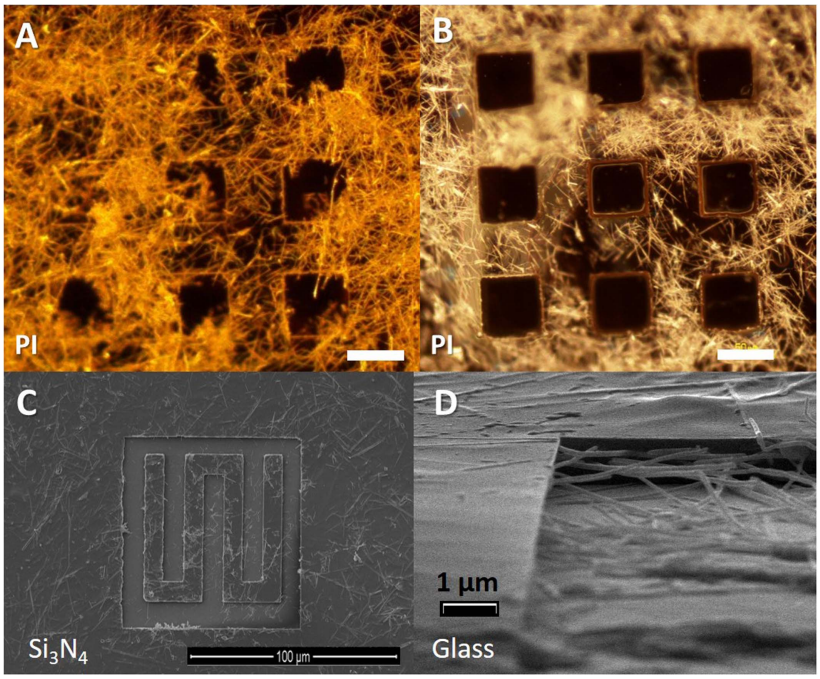


**Figure 5.** Images of EBL on AgNWs-PMMA applied over insulating substrates. Optical images in dark field mode on polyimide (PI) film before (A) and after (B) silver etching; scale bar = 50 $\mu$m. SEM images of EBL patterns on silicon substrate covered with a $Si_3N_4$ layer (C) and on glass (D) after silver etching.

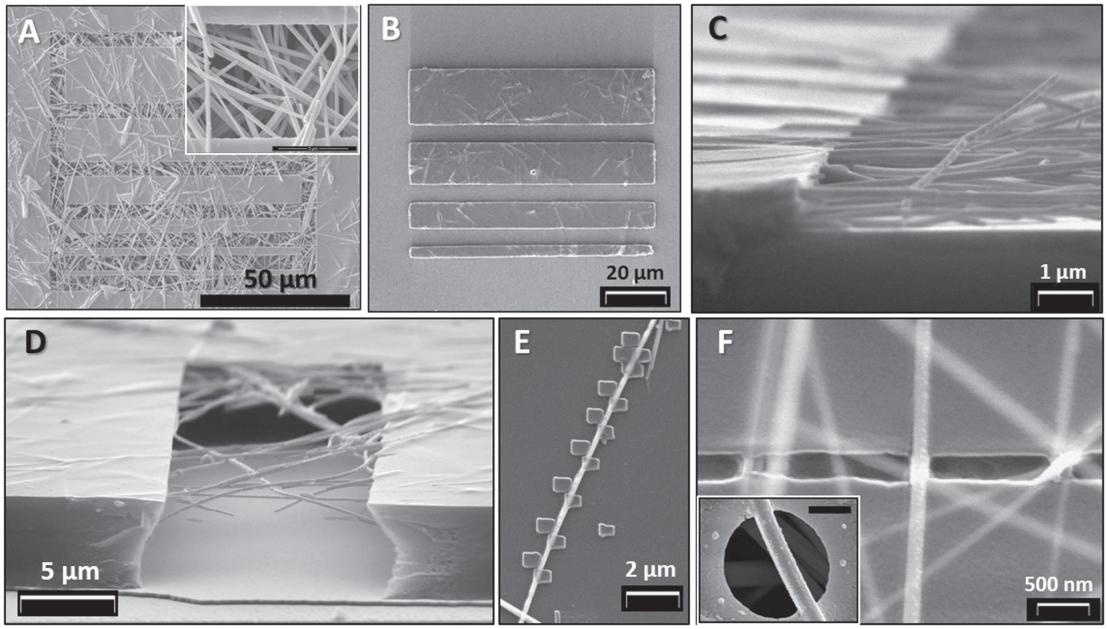


**Figure 6.** SEM image of nanowires structures formed by EBL. Conductive stripes before silver etching (A) with the AgNWs network underneath shown in the inset. (B) Conductive strips after silver etching. (C) Lateral view of AgNWs-PMMA nanocomposite resist after EBL. (D) AgNWs bridges in a multilayer PMMA-AgNWS/PMMA. (E) Local covering of a single AgNW in specific regions and local release of a small portion of AgNWs across a line (F), inset: suspended AgNWs in lithographic defined circular hole (scale bar: 500 nm).

stamped resistor was measured with two contact probes (figure 7(B)). It was observed that when using the nanocomposite resist with more than 1.5%wt of AgNWs a percolated network of pressed wires remains on the surface in the undesired regions, short-circuiting the pads; therefore, lower mass fractions of AgNWs must be used in the resist. Interestingly, by modifying the synthesis of AgNWs by introduciong KBr as a growth control [33], we were able to produce AgNWs with thinner diameters (approximately 100 nm) but similar lengths. In this way, we could reduce the silver content in the

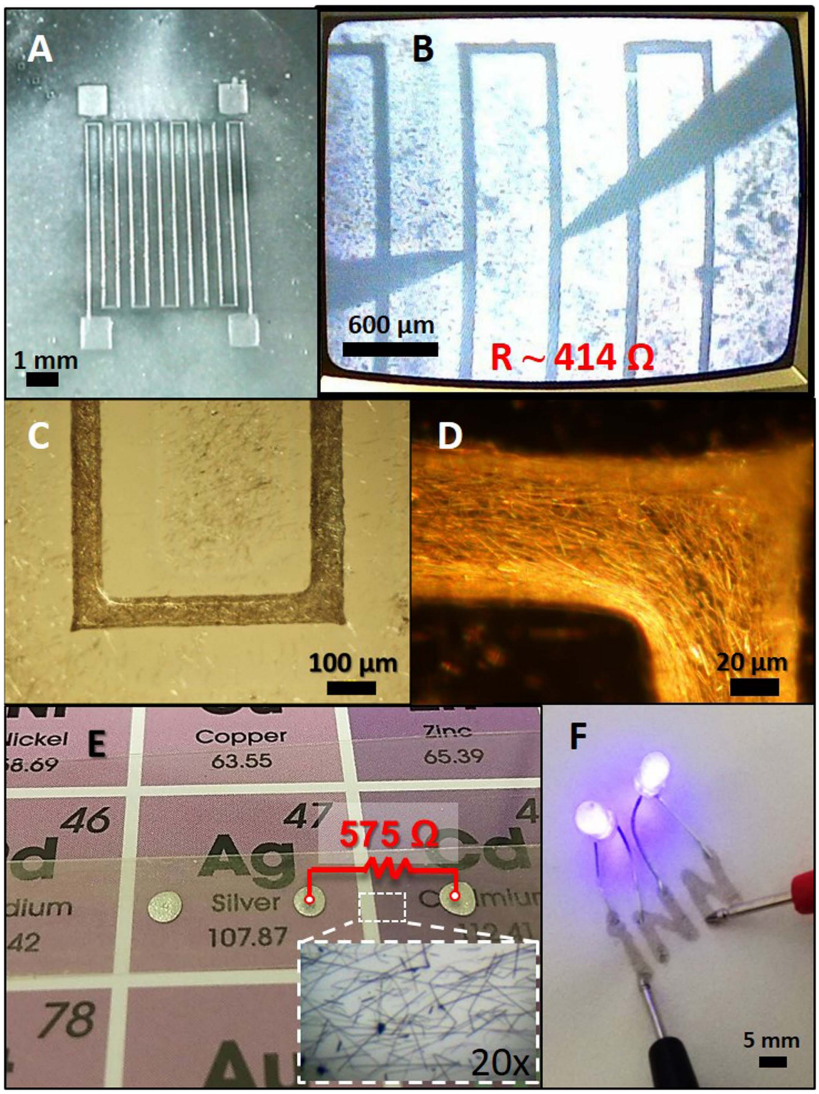


**Figure 7.** (A) Resistor device on a PET substrate made by soft lithography. (B) Picture of a local 2-probes measurement of conductive tracks. Optical images of conductive tracks in bright field mode (C) and dark field mode (D). An example of a transparent film made with the AgNWs-PMMA resist on a PET sheet (E) and the resistance measured between contacts of silver paste. The inset shows an optical image of the network of NWs on the indicated area, objective lens 20X, ocular lens 10X. (F) Conductive patterns drawn by hand with 1.5%wt AgNWs-PMMA ink.

nanocomposite resist to only 0.4%wt to produce thin films of the resist with high transparency and fair electrical conductance (see figure 7(E)). Current efforts are underway to complete the study on transparent devices made with this resist containing AgNWs with higher aspect ratios. Regarding the mechanical properties and specifically the bendability of the nanocomposite films on flexible substrates, it is worth to mention that for the case of ITO, its elongation before fracture (strain limit) on flexible substrates was studied to be 1.59% [1]. On the other hand, PMMA films have shown a higher strain limit, ranging from 3% [34] to nearly 20% [35]. In fact, our observations and preliminary tests have shown that the nanocomposite films deposited on polyimide tape (50 $\mu$m thick) can be bent without cracking along a curvature radius of 2.5 mm. Considering that the strain produced in the outer layer of the film, $\varepsilon_f$, during bending can be calculated as $\varepsilon_f = (d_f + d_s)/2R$, where $d_f$ is the film thickness (3 $\mu$m in our case), $d_s$ is the thickness of the substrate, and $R$ the bending radius, it is possible to conclude from the elongation produced, $\varepsilon_f \sim 1.1\%$, that the mechanical properties of PMMA based nanocomposites are suitable enough for flection.

Finally, the nanocomposite resist was tested as a conductive ink. Using a resist with 1.5%wt content of AgNWs, a conductive track was drawn by hand on a filter paper and dried at room temperature for about two minutes. The electrical conductance was demonstrated by contacting two blue light LEDs and applying a bias potential of 5 V at the ends of the tracks (figure 7(F)). Recent works have reported the importance of AgNWs based conductive inks and suggested the incorporation of additives to favor its use for inkjet printing [36–38].

## 4. Conclusion

In summary, we provide a novel multifunctional nanocomposite resist based on AgNWs dispersed in a solution of a high molecular weight PMMA. We have provided evidence for the suitability of this composite material in microfabrication by applying different techniques. These include EBL as a proper way to achieve high resolution and low dimension devices, but also by soft lithography, which provides an economical way to scale up fabrication processes. The application of this nanocomposite resist for EBL provides a simple way to overcome electrical charging problems when using this technique on insulating substrates. In this case, the nanocomposite resist could merely serve as a sacrificial material. In addition, either EBL and soft lithography can now be applied on flexible substrates, forming conductive patterns for next-generation technology of flexible electronics. Lastly, the simple formulation proposed for this nanocomposite resist allows its use as a conductive ink, similar to the ones commonly employed in electronics workshops, labs and in the industry, but containing remarkable lower silver fraction (1.5%wt) compared to commercially available silver paints and pastes (>30%wt). It is important to notice the potential of this nanocomposite material since the synthesis parameters can be optimized, maybe including growth control agents such as KBr (as mentioned) to reduce the diameter of the AgNWs and enlarge their aspect ratio [33]. This was shown to provide a nanocomposite material with the same electrical performance but with lower optical density, therefore, forming transparent and conductive devices with lower silver content. The possibility of alignment of AgNWs must be considered as well since many different procedures have recently been reported on this topic [39–44], opening new applications for nano and microdevices. In addition, using EBL on AgNWs-PMMA nanocomposites opens a brand new range of opportunities for anchoring and exploiting single AgNWs, arrange multilayer structures to form suspended arrays of AgNWs and exposing specific parts of the nanowires to the environment for functionalization and selective deposition of other materials. For example, the plasmonic properties of AgNWs [45–47] could be studied and exploited using EBL as a simple way to manipulate single AgNWs. Given the features displayed by the AgNWs-PMMA nanocomposite resist, it is concluded that in the road to transparent, flexible an complex electronics this material offers new and exciting opportunities.

## Acknowledgments

We thank Daniel O Wilberger and Dr Horacio Troiani from Materials Department at CAB-CNEA for their assistance in Field Emission SEM and HR-TEM imaging respectively. Special thanks to Virginia Tognolli for the preparation of tungsten needles probes. We thank Dr Leonardo Salazar-Alarcón and Julián Azcárate for their cooperation and Dr Nestor Haberkorn, also from Low Temperature Physics Division at CAB-CNEA, for his assistance in *I–V* curves acquisition. Funding was provided by ANPCyT PICT 2012/770, PICT 2011/752, PIP CONICET 0490 and SECyT-UNCuyo 06/C456 and Instituto de Nanociencia y Nanotecnología (INN). EDM acknowledges a postdoctoral fellowship from CONICET, JL acknowledges a doctoral fellowship from CONICET.

## References

[1] Peng C, Jia Z, Bianculli D, Li T and Lou J 2011 *J. Appl. Phys.* **109** 103530
[2] Bergin S M, Chen Y H, Rathmell A R, Charbonneau P, Li Z Y and Wiley B J 2012 *Nanoscale* **4** 1996
[3] Langley D, Giusti G, Mayousse C, Celle C, Bellet D and Simonato J P 2013 *Nanotechnology* **24** 452001
[4] Anh Dinh D, Nam Hui K, San Hui K, Singh J, Kumar P and Zhou W 2013 *Rev. Adv. Sci. Eng.* **2** 324–45
[5] José Andrés L, Fe Menéndez M, Gómez D, Luisa Martínez A, Bristow N, Paul Kettle J, Menéndez A and Ruiz B 2015 *Nanotechnology* **26** 265201
[6] Langley D P, Giusti G, Lagrange M, Collins R, Jiménez C, Bréchet Y and Bellet D 2014 *Sol. Energy Mater. Sol. Cells* **125** 318–24
[7] Noh Y J, Kim S S, Kim T W and Na S I 2013 *Semicond. Sci. Technol.* **28** 125008
[8] Chiamori H, Brown J, Adhiprakasha E, Hantsoo E, Straalsund J, Melosh N and Pruitt B 2008 *Microelectron. J.* **39** 228–36
[9] Hanemann T and Szabó D V 2010 *Materials* **3** 3468–517
[10] Suter M, Ergeneman O, Zürcher J, Schmid S, Camenzind A, Nelson B J and Hierold C 2011 *J. Micromech. Microeng.* **21** 025023
[11] Damean N, Parviz B A, Lee J N, Odom T and Whitesides G M 2005 *J. Micromech. Microeng.* **15** 29–34
[12] Jiguet S, Bertsch A, Hofmann H and Renaud P 2004 *Adv. Eng. Mater.* **6** 719–24
[13] Jiguet S, Bertsch A, Hofmann H and Renaud P 2005 *Adv. Funct. Mater.* **15** 1511–6
[14] Ingrosso C, Fakhfouri V, Striccoli M, Agostiano A, Voigt A, Gruetzner G, Curri M L and Brugger J 2007 *Adv. Funct. Mater.* **17** 2009–17
[15] Kandpal M, Sharan C, Poddar P, Prashanthi K, Apte P R and Ramgopal Rao V 2012 *Appl. Phys. Lett.* **101** 104102
[16] Balamurugan A, Ho K C and Chen S M 2009 *Synth. Met.* **159** 2544–9
[17] Myers A C, Huang H and Zhu Y 2015 *RSC Adv.* **5** 11627–32
[18] Tamboli M S, Kulkarni M V, Patil R H, Gade W N, Navale S C and Kale B B 2012 *Colloids Surf.* B **92** 35–41
[19] Choi S *et al* 2015 *ACS Nano* **9** 6626–33
[20] Zhou Y N, Cheng H and Luo Z H 2013 *AIChE J* **59** 4780–93
[21] Vinchurkar M, Joshi A, Pandey S and Rao V R 2015 *J. Microelectromech. Syst.* **24** 1111–6
[22] Hong K, Yang C, Kim S H, Jang J, Nam S and Park C E 2009 *ACS Appl. Mater. Interfaces* **1** 2332–7
[23] Jiang L, Spearing S, Monclus M and Jennett N 2011 *Compos. Sci. Technol.* **71** 1301–8
[24] Grimaldi C, Mionic M, Gaal R, Forro L and Magrez A 2013 *Appl. Phys. Lett.* **102** 223114
[25] Satyalakshmi K M, Olkhovets A, Metzler M G, Harnett C K, Tanenbaum D M and Craighead H G 2000 *J. Vac Sci. Technol.* B **18** 3122
[26] Liu W 1995 *J. Vac Sci. Technol.* B **13** 1979

[27] Cummings K D 1990 *J. Vac Sci. Technol.* B **8** 1786
[28] Guo L J 2007 *Adv. Mater.* **19** 495–513
[29] Jiu J *et al* 2014 *J. Mater. Chem.* A **2** 6326
[30] Schroder D K 2006 *Semiconductor Material and Device Characterization* 3rd edn (Hoboken, NJ: Wiley-IEEE Press)
[31] Xia Y N and Whitesides G M 1998 *Angew. Chem. Int. Ed. Engl.* **37** 551–75
[32] Qin D, Xia Y and Whitesides G M 2010 *Nat. Protocols* **5** 491–502
[33] Zhang K, Du Y and Chen S 2015 *Org. Electron.* **26** 380–5
[34] Abdel-Mohti A, Garbash A, Almagahwi S and Shen H 2015 *Materials* **8** 2062–75
[35] Cheng W M, Miller G A, Manson J A, Hertzberg R W and Sperling L H 1990 *J. Mater. Sci.* **25** 1917–23
[36] Wu J T, Lien-Chung Hsu S , Tsai M H, Liu Y F and Hwang W S 2012 *J. Mater. Chem.* **22** 15599
[37] Chen S P, Durán Retamal J R, Lien D H, He J H and Liao Y C 2015 *RSC Adv.* **5** 70707–12
[38] Nair K G, Jayaseelan D and Biji P 2015 *RSC Adv.* **5** 76092–100
[39] Duan S K, Niu Q L, Wei J F, He J B, Yin Y A and Zhang Y 2015 *Phys. Chem. Chem. Phys.* 8106–12
[40] Yang B R, Cao W, Liu G S, Chen H J, Noh Y Y, Minari T, Hsiao H C, Lee C Y, Shieh H P D and Liu C 2015 *ACS Appl. Mater. Interfaces* **7** 21433–41
[41] Cao Y, Liu W, Sun J, Han Y, Zhang J, Liu S, Sun H and Guo J 2006 *Nanotechnology* **17** 2378–80
[42] Xu F, Durham J W, Wiley B J and Zhu Y 2011 *ACS Nano* **5** 1556–63
[43] Shi H Y, Hu B, Yu X C, Zhao R L, Ren X F, Liu S L, Liu J W, Feng M, Xu A W and Yu S H 2010 *Adv. Funct. Mater.* **20** 958–64
[44] Ma X, Zhu X, You F, Feng J, Wang M C and Zhao X 2014 *J. Alloys Compd.* **592** 57–62
[45] Pyayt A L, Wiley B, Xia Y, Chen A and Dalton L 2008 *Nat. Nanotechnol.* **3** 660–5
[46] Wild B, Cao L, Sun Y, Khanal B P, Zubarev E R, Gray S K, Scherer N F and Pelton M 2012 *ACS Nano* **6** 472–82
[47] Xiong X, Zou C L, Ren X F, Liu A P, Ye Y X, Sun F W and Guo G C 2013 *Laser Photon Rev.* **7** 901–19